RSC Advances

PAPER

View Article Online
View Journal | View Issue

Cite this: *RSC Adv.*, 2024, **14**, 15031

Achievement of waste sludge deep dehydration under acidic conditions with polydimethyldiallylammonium chloride and ferric chloride: performance and mechanism

Yong-Tao Lv, [abc] Kaichong Wang,[abc] Jiaxin Liu,[abc] Xudong Wang,[abc] Le Li,[abc] Junqi Qiu[a] and Lei Wang *[abc]

The biological treatment of wastewater generates a substantial amount of waste sludge that requires dewatering before final disposal. Efficient sludge dewatering is essential to minimize storage and transportation costs. In this study, the sludge conditioners polydimethyldiallylammonium chloride (PDMDAAC) and ferric chloride ($FeCl_3$) were sequentially dosed, and the pH was adjusted to 3. As a result, the sludge moisture content (MC) was reduced to 59.4%, achieving deep dewatering. After conditioning, the tightly bound extracellular polymeric substances (TB-EPS) were reduced from 34.5 to 10.2 mg g^{-1} VSS, with the majority of the reduced fractions being composed of protein (PN). In contrast, soluble EPS increased more than 8 times. Subsequent studies revealed that the decrease in PN from TB-EPS primarily involved tryptophan and tyrosine proteins, accompanied by a significant reduction in the N–H and C=C absorption peaks. These results highlight the critical role of TB-EPS dissolution in achieving deep dehydration, with the N–H in PN was identified as the key group influencing sludge dewatering. Combined with the changes in sludge particle size and morphology, the dewatering mechanism can be summarized as follows: PDMDAAC dissolves TB-EPS, simultaneously disrupting the floc structure and refining the sludge. Subsequently, $FeCl_3$ reconstructs these elements, forming larger particle sizes. Finally, hydrochloric acid reduces TB-EPS once again, releasing bound water. This study offers alternative methods and new insights for achieving deep dewatering of waste sludge.

Received 20th February 2024
Accepted 1st May 2024

DOI: 10.1039/d4ra01311e

rsc.li/rsc-advances

1. Introduction

The activated sludge process is the most widely used method for wastewater treatment, playing an important role in purifying wastewater and improving water environments.[1] However, it inevitably generates a significant amount of waste sludge.[2,3] These sludges contain a substantial amount of organic matter and must be appropriately disposed of (*e.g.*, landfill or incineration) to prevent secondary pollution of soil and groundwater.[4–6] Due to their high moisture content (MC), sludge dewatering is necessary before disposal to reduce the storage and transportation costs.[7,8] To enhance the efficiency of sludge dewatering, chemical reagents are commonly introduced for conditioning.[3,7,9] Traditional chemical conditioning agents, such as polymeric $FeCl_3$, polymeric aluminum chloride, and polyacrylamide, work to improve sludge dewatering performance by primarily removing free water through electrical neutralization and bridging mechanisms.[10,11] However, they face limitations as they cannot effectively release the bound water within the sludge, restricting their effectiveness in achieving deep dehydration.[12]

Extracellular polymeric substances (EPS) are organic polymers secreted by microorganisms, tightly bound to water molecules through chemical bonding, thereby influencing the deep dewatering of sludge.[13–15] Previous studies have demonstrated that advanced conditioning processes, such as oxidation and heat treatment, can disrupt the EPS structure, releasing bound water and effectively improving sludge dewatering performance.[16,17] However, the high treatment cost and harsh operating conditions associated with these methods limit their large-scale applications.

Surfactants have been identified as agents capable of dissolving EPS, but their impact on sludge dewatering remains a topic of debate. Ye *et al.* found that sodium dodecyl sulfate can release EPS from sludge, but this led to a deterioration in sludge dewatering performance.[9,18] In contrast, He *et al.* observed that

[a]*School of Environmental and Municipal Engineering, Xi'an University of Architecture and Technology, No. 13 Yanta Road, Xi'an 710055, China. E-mail: wl0178@126.com; Tel: +86 2982202729*

[b]*Key Laboratory of Membrane Separation of Shaanxi Province, Research Institute of Membrane Separation Technology of Shaanxi Province, No. 13 Yanta Road, Xi'an 710055, China*

[c]*Key Laboratory of Environmental Engineering of Shaanxi Province, No. 13 Yanta Road, Xi'an 710055, China*

the sequential addition of polydimethyldiallylammonium chloride (PDMDAAC) and tannic acid enhanced sludge dewatering performance, reducing the MC to 67.8%.[16] These differences highlight the challenge of achieving optimal dewatering performance using surfactants alone. Consequently, exploring the combined use of surfactants is anticipated to offer new insights for enhancing sludge dewatering. In addition, EPS components and structure are complex, with extracellular protein (PN) and exopolysaccharide (PS) collectively accounting for 70–80%.[19] EPS exhibits spatial layering characteristics, divided into tightly bound EPS (TB-EPS), loosely bound EPS (LB-EPS), and soluble EPS (S-EPS) in order from the inside to the outside.[20,21] However, the component that plays a dominant role in sludge dewatering (PS or PN), as well as the spatial subcomponent (TB-EPS, LB-EPS, or S-EPS), remains to be further clarified.[22–25]

In this study, PDMDAAC, ferric chloride ($FeCl_3$), and HCl were utilized as conditioning agents for achieving deep sludge dewatering. Initially, the effects of different combinations on sludge MC and capillary suction time (CST) were examined to determine the optimal parameters. Simultaneously, variations in EPS components and structures, sludge surface properties, and morphology during the conditioning process were characterized and correlated with the sludge dewatering performance. The goal is to provide alternative methods and new insights for realizing deep sludge dewatering.

2. Materials and methods

2.1. Chemical reagents

In this study, PDMDAAC, $FeCl_3$ and HCl were used as sludge conditioners, and all three were of analytical purity. PDMDAAC and $FeCl_3$ were procured from Shanghai Aladdin Biochemical Technology Co., while HCl was obtained from Sinopharm Chemical Reagent Co. In addition, the bovine serum albumin (BSA) and glucose used in the experiments were analytically pure and were obtained from Tianjin Komeo Chemical Reagent Co.

Table 1 Characteristics of the original sludge

pH		6.7 ± 0.2
WC (%)		98.0 ± 2.0
Zeta potential (mV)		−19.76 ± 2.0
Particle size (μm)		43.61 ± 2.0
CST (s)		84.2 ± 3.0
PN (mg g^{-1} VSS)	TB-EPS	30.72 ± 1.73
	LB-EPS	0.82 ± 0.09
	S-EPS	1.36 ± 0.03
PS (mg g^{-1} VSS)	TB-EPS	12.13 ± 1.32
	LB-EPS	0.35 ± 0.01
	S-EPS	0.34 ± 0.01

2.2. Wasted sludge sources and dewatering tests

The wasted sludge was obtained from the 5th Wastewater Treatment Plant in Xi'an, with specific characteristics detailed in Table 1. Sludge samples were collected and tested on the same day. Initially, 500 mL of sludge was sampled and placed in a beaker. The conditioner was then added, and the mixture was stirred using a magnetic stirrer (KDM thermoregulation type, Huaru Electric Heating Apparatus, Shandong, China) for 10 min. Subsequently, the mixture was poured into a filter bag (180 × 430–0.5 micron, Bifilter, Zhejiang, China), hand-twisted until no more water dripped, and the MC of the sludge was determined. Each test was conducted three times.

The optimal dosage of PDMDAAC, $FeCl_3$, and HCl was determined individually at 0.375 g g^{-1} dry sludge (DS), 2.0 g g^{-1} DS, and pH 3.0, respectively. Subsequent tests (Table 2) were conducted to identify the optimum dewatering parameters.

2.3. Conventional analytical methods

The sludge MC was determined using the drying and weighing method,[26] while the CST was measured using a portable CST tester (CST DP-304B, Asia-Eurodepen Technology, Beijing, China). The pH of the sludge samples was measured with a standard acidity meter (ST2100, Ohaus, New Jersey, US). The zeta potential and particle size of the sludge were determined using a zeta potential meter (ZS90, Malvern PANalytical, Malvern, UK) and a laser particle size distribution meter (Sync, Microtrac, Pennsylvania, US), respectively. Sludge morphology was examined using scanning electron microscopy (SEM) (JSM-6510LV, JEOL, Tokyo, Japan) after the samples underwent dehydration and plating.

2.4. EPS extraction and analysis

2.4.1. Determination of EPS components. Total EPS was extracted from sludge samples using a modified heating method. The extraction of each EPS subfraction (*i.e.*, S-EPS, LB-EPS, and TB-EPS) followed the procedure outlined by Wang *et al.*[27] The analysis of PN and PS contents in the extracted EPS was conducted using the method described by Frølund *et al.*[28] The concentrations of PN and PS were determined using BSA and glucose as standards, respectively.

2.4.2. Analysis of fluorescent substances in EPS. The composition of fluorescent substances in the EPS subfractions was determined using a three-dimensional excitation-emission

Table 2 Waste sludge dewatering test program

	Sludge conditioning agents		
No.	PDMDAAC (g g^{-1} DS)	$FeCl_3$ (g g^{-1} DS)	pH
1	0.375	0, 0.5, 1.0, 1.5, 2.0, 2.5	7.0
2	0, 0.125, 0.25, 0.375, 0.5, 0.625	2.0	7.0
3	0.375	2.0	7.0, 6.0, 5.0, 4.0, 3.0, 2.0

matrix (3D-EEM). Pre-processing of the S-EPS involved using a filter with a pore size of 0.22 μf. The excitation wavelengths ranged from 200 to 500 nm at 3 nm intervals, and the emission wavelengths ranged from 250 to 550 nm at 3 nm intervals. The scanning speed and voltage of the photomultiplier tube were set at 12 000 nm min^{-1} and 600 V, respectively.

Absorption peaks in the 3D-EEM include the following components: tyrosine-like proteins (Ex, 220–250 nm; Em, 280–330 nm); tryptophan-like proteins (Ex, 220–250 nm; Em, 330–380 nm); xanthic acid-like organics (Ex, 240–255 nm; Em, 380–550 nm); microbial-like by-product material (Ex, 250–450 nm; Em, 280–380 nm); humic acid-like organics (Ex, 340–450 nm; Em, 380–550 nm).

2.4.3. Analysis of EPS subfraction functional groups. Samples of both raw sludge and conditioned sludge (PDMDAAC + $FeCl_3$ + HCl) were collected, freeze-dried, and mixed with FTIR spectral grade KBr powder at a mass ratio of 100 : 1. To analyze the major functional groups of the three EPS subfractions, FTIR spectra of EPS were obtained using a FTIR spectrometer (Nicolet 5700, Applied Separations, USA) with wavenumbers ranging from 500 cm^{-1} to 4000 cm^{-1}.[29]

2.5. Statistical analysis

Statistical analysis was carried out by using the software of SPSS version 19.0. Correlations are considered statistically significant at 95% confidence interval ($p < 0.05$).

3. Results and discussion

3.1. Variation in sludge dewatering performance

The sludge MC and CST exhibited a decreasing and then increasing trend with the increase in PDMDAAC dosage (Fig. 1a). As the PDMDAAC dosage increased from 0 to 0.375 g g^{-1} DS, the sludge MC decreased from 74.86% to the minimum 64.81%, accompanied by a decrease in CST from 71.85 s to 22.00 s. This suggests that a low dosage of PDMDAAC effectively reduces the MC of the sludge and enhances its water permeability. However, dosages exceeding 0.375 g g^{-1} DS led to an increase in sludge viscosity,[11] resulting in higher CST and posing challenges for dewatering.

The sludge dewatering performance exhibited a trend of increasing and then decreasing with the rise in $FeCl_3$ dosage (Fig. 1b). At a dosage of 2.0 g g^{-1} DS, the sludge MC decreased to 64.91%, and the CST was 21.85 s, representing the optimal dewatering performance. However, when the dosage exceeded 2.0 g g^{-1} DS, noth the sludge MC and CST decreased, indicating a decline in sludge dewatering performance. The excessive $FeCl_3$ appeared to impact the aggregation performance of the sludge and could potentially disrupt its structure, thereby affecting dewatering performance.[30]

The sludge MC tends to decrease and then increase with decreasing pH from 7.0 to 2.0 (Fig. 1c), aligning with the findings from He *et al.* who studied sludge dewatering using PDMDAAC in combination with tannic acid.[16] The acidic conditions lower the negative charge of the sludge, destabilizing it. Furthermore, acidification can potentially disrupt the sludge structure and even induce cell lysis.[31,32] Additionally, the acidic pH is known to reduce the viscosity of the polymer, enhancing the water permeability of the sludge.[8,33]

In summary, the sludge MC could be reduced to 64.8% by using PDMDAAC and $FeCl_3$ as sludge conditioners. Building upon this, the addition of HCl to adjust the pH to 3.0 further lowered the sludge MC to 59.4%, achieving deep dewatering of the sludge.

3.2. Variation in EPS before and after sludge conditioning

3.2.1. Variation in EPS components and contents. The total EPS decreased from 39.6 to 30.1 mg g^{-1} VSS with the increase in PDMDAAC dosage (Fig. 2a). Among the subfractions, TB-EPS was the primary contributor to the reduction in total EPS, decreasing from 34.5 to 25.9 mg g^{-1} VSS. PDMDAAC, with its amphiphilic structure, demonstrated the ability to dissolve EPS,

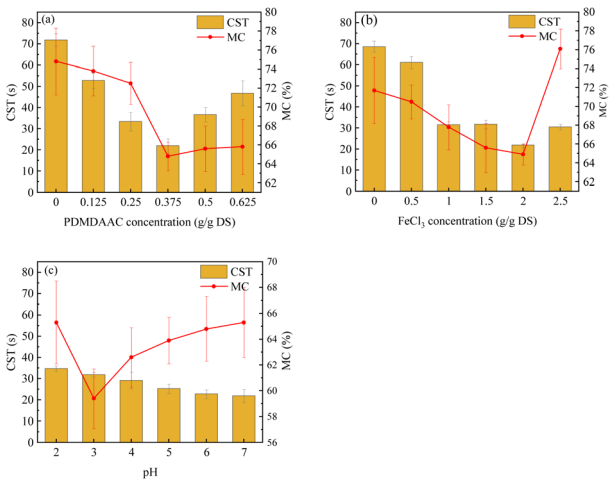

Fig. 1 Variation of sludge MC and CST under different conditions: (a) $FeCl_3$ dosage of 2.0 g g^{-1} DS; (b) PDMDAAC dosage of 0.375 g g^{-1} DS; (c) PDMDAAC and $FeCl_3$ at 0.375 and 2.0 g g^{-1} DS, respectively.

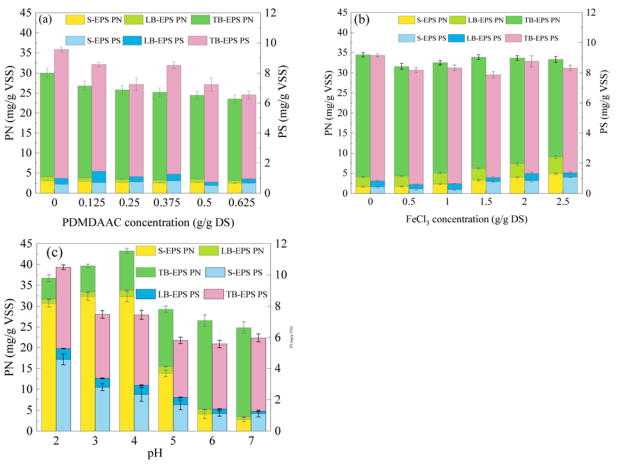

Fig. 2 Variation of EPS components and contents under different conditions: (a) $FeCl_3$ dosage of 2.0 g g^{-1} DS; (b) PDMDAAC dosage of 0.375 g g^{-1} DS; (c) PDMDAAC and $FeCl_3$ at 0.375 and 2.0 g g^{-1} DS, respectively.

specifically converting TB-EPS to S-EPS.[34] This study further supports the notion that PDMDAAC can effectively reduce total EPS. Regarding EPS content, both PN and PS decreased by 6.5 and 3.0 mg g^{-1} VSS, respectively, with the former being the main contributor to the EPS reduction, accounting for 68.4%.

The impact of $FeCl_3$ on total EPS (39.8–43.6 mg g^{-1} VSS) was less pronounced compared to PDMDAAC (Fig. 2b). With increasing $FeCl_3$ dosage, TB-EPS decreased from 38.7 to 31.2 mg g^{-1} VSS. In contrast, both LB-EPS and S-EPS increased, rising from 2.8 and 2.1 to 4.4 and 5.9 mg g^{-1} VSS, respectively. Considering the acidic nature of $FeCl_3$, the increase in dosage led to the production of hydrogen ions, which in turn dissolved TB-EPS into LB-EPS and S-EPS.[34]

The EPS increased dramatically when the pH was decreased from 7.0 to 2.0 (Fig. 2c), reaching a maximum of 50.7 mg g^{-1} VSS at pH 4, where the PNs rose to 43.3 mg g^{-1} VSS, marking a 1.7 times increase compared to pH 7. The strongly acidic pH caused cell lysis, leading to the release of intracellular substances,[35–37] as evident from the significant increase in PNs. Additionally, with decreasing pH (from 7 to 2), TB-EPS decreased from 26.1 to 10.2 mg g^{-1} VSS, and the major decrease was attributed to PNs. In contrast, S-EPS increased drastically from 3.9 to 35.3 mg g^{-1} VSS, representing more than 8-fold increase. The conditioning method employed in this study promoted a significant dissolution of TB-EPS, resulting in the achievement of deep dehydration in the sludge (Fig. 1c).[38–40]

EPS, with its water-holding function, was highlighted in this study, emphasizing that TB-EPS played a key role in influencing sludge dewatering. Positioned in the inner layer of the sludge, the dissolution of TB-EPS was found to release bound water, thereby positively contributing to enhanced sludge dewatering.[41] Notably, the optimal sludge dewatering performance did not coincide when the minimum TB-EPS content, indicating that its content alone was not the sole factor influencing sludge

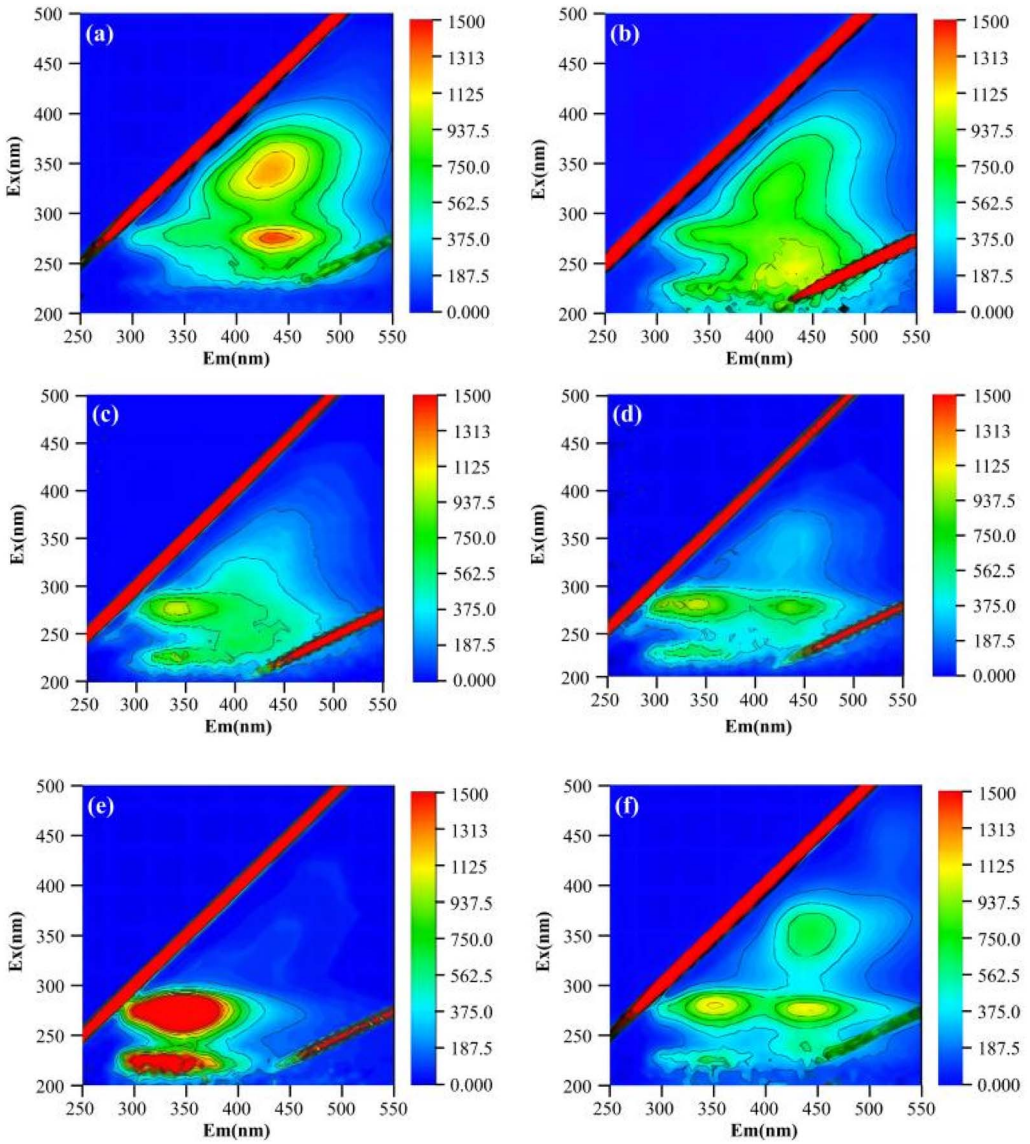

Fig. 3 Variation in fluorescence substances in EPS, where (a, c and e) represent S-EPS, LB-EPS, and TB-EPS of the original sludge; and (b, d and f) represent S-EPS, LB-EPS, and TB-EPS of the sludge after conditioning.

dewatering performance. Moreover, the reduction in TB-EPS observed in this study was predominantly attributed to PN, suggesting that PN is a key component affecting sludge dewatering.

3.2.2. Variation of fluorescent substances in EPS. The main fluorescent substances in the original sludge include tyrosine-like proteins, tryptophan-like proteins, and microbial byproducts (Fig. 3e). After conditioning, the fluorescence peak intensity decreased, with the absorption peak of tyrosine-like protein essentially disappearing and the peak strength of tryptophan-like protein greatly weakened (Fig. 3f), aligning with the significant decrease in PNs content (Fig. 2c). The 3D-EEM results further confirmed that the decreased PNs in this study were tyrosine and tryptophan proteins. In contrast, the S-EPS spectrum revealed that after sludge conditioning, a tyrosine-like protein absorption peak appeared, and the absorption peak of tryptophan-like protein was significantly enhanced (Fig. 3a and b). This suggests that the increased PNs in S-EPS are also tyrosine and tryptophan proteins. In contrast, there was no obvious change in the peak intensity of fluorescent proteins in LB-EPS before and after conditioning (Fig. 3c and d).

Furthermore, compared with the original sludge, both TB-EPS and LB-EPS contain higher amounts of humic acid organic compounds. These compounds are likely released from intracellular organic matter due to cell lysis.[42–44] However, there is currently no evidence to certify that changes in humic acid are associated with sludge dewatering.

3.2.3. Variation in EPS functional groups. As illustrated in Fig. 4, the primary functional groups in EPS include the N–H functional group (found in the 3450–3400 cm^{-1} band), C=O (amide I), and the C=C functional group (located in the 1660–1630 cm^{-1} band) in PNs. Additionally, EPS includes the C=C functional group in carbohydrates (within the 1300–1500 cm^{-1} band) and the C–OH and C–O–C functional groups in PS (within the 1080–1030 cm^{-1} band).[45]

After conditioning, LB-EPS exhibited no significant changes in its characteristic peaks, except for a slight weakening of the N–H absorption peak at 3432 cm^{-1}. Conversely, the absorption peaks of S-EPS were all enhanced, particularly the C=C functional group at 1628 cm^{-1} and C–OH at 1079 cm^{-1}, indicating an increase in soluble PN and PS. In contrast, the absorption peaks of TB-EPS were significantly weakened, especially the N–H (3432 cm^{-1}) and C=C functional groups (1628 cm^{-1}) in PNs. This aligned with the sharp decrease in the content of PNs in TB-EPS (Fig. 2c). Since C=C is a hydrophobic functional group, in this study, the functional group affecting sludge dewatering is N–H. This highly hydrophilic functional group has a more substantial effect on the water-holding capacity of the EPS compared to, for example, C=O and OH–.[46] When present in TB-EPS, they can effectively lock water through hydrogen bonds.[47,48]

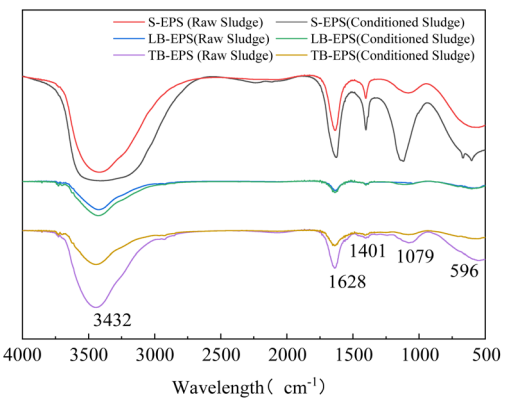

Fig. 4 Variation of the functional groups in EPS before and after conditioning.

3.3. Changes in sludge characteristics

3.3.1. Changes in sludge particle size. The particle size of the sludge initially increased and then slightly decreased with an increase in either PDMDAAC or $FeCl_3$ dosage (Fig. 5a and b).[11,49] Notably, this study revealed that $FeCl_3$ had a more pronounced impact on sludge particle size compared to PDMDAAC, leading to an increase from 41.8 to 50.0 μm (Fig. 5b). Interestingly, the largest sludge particle size corresponded to the smallest sludge MC and CST, suggesting a close relationship between sludge particle size and dewatering performance. When the sludge aggregates to form larger particles, it facilitates the removal of free water among flocs and prevents clogging of the filter cloth, thereby enhancing water permeability performance.[22,41,50]

The sludge particle size exhibited a continuous decrease as the pH was decreased from 7 to 2 (Fig. 5c), reaching a minimum value of 46.3 μm. This trend elucidates the observed increase in CST as the pH decreased (Fig. 1c). Overall, the pH exerted little influence on the sludge particle size, indicating the formation of a more stable large particle size structure after conditioning with PDMDAAC and $FeCl_3$. Despite the TB-EPS at pH 2 being reduced to a minimum (Fig. 2c), the structural disruption of sludge aggregates and the concurrent reduction in particle size both increased the challenges associated with sludge dewatering.

3.3.2. Changes in zeta potential at the sludge surface. Zeta potential is an important indicator to describe the flocculation and dispersion characteristics of sludge.[14,51] PDMDAAC, a cationic surfactant, and $FeCl_3$, a coagulant, both contribute to an increase in Zeta potential through electrical neutralization ($P < 0.05$) (Fig. 6a and b). Consequently, the electrostatic repulsion is reduced, leading to the formation of larger sludge particles through aggregation.[4,52] The addition of HCl also elevates zeta potential through electro-neutralization ($P < 0.05$) (Fig. 6c). When the pH falls below the isoelectric point of the sludge, the zeta potential becomes positive. Notably, at a pH of 2, the zeta potential rises to 7.48 mV, increasing the repulsive force between sludge particles. Simultaneously, this decrease in pH disrupts the sludge structure, induces cell lysis, and contributes to the reduction in sludge particle size, ultimately deteriorating dewatering performance.

3.3.3. Changes in sludge morphology. The surface structure of the original sludge appeared loose and amorphous

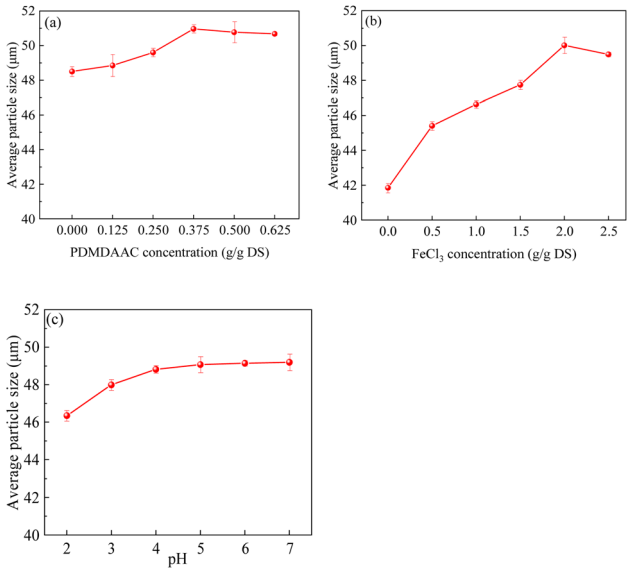

Fig. 5 Variation in sludge particle size under different conditions: (a) $FeCl_3$ dosage of 2.0 g g^{-1} DS; (b) PDMDAAC dosage of 0.375 g g^{-1} DS; (c) PDMDAAC and $FeCl_3$ dosages of 0.375 and 2.0 g g^{-1} DS, respectively.

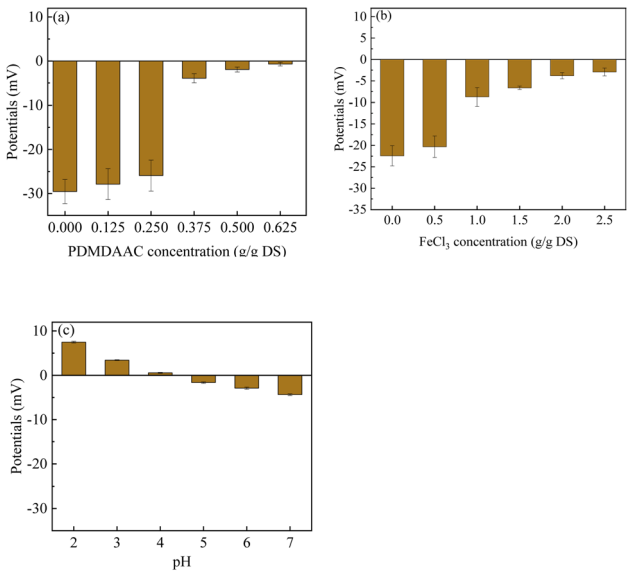

Fig. 6 Variation in zeta potential under different conditions: (a) $FeCl_3$ dosage of 2.0 g g^{-1} DS; (b) PDMDAAC dosage of 0.375 g g^{-1} DS; (c) PDMDAAC and $FeCl_3$ dosages of 0.375 and 2.0 g g^{-1} DS, respectively.

(Fig. 7a), making the removal of free water and bound water challenging and resulting in weak dewatering performance. Upon the addition of PDMDAAC or HCl alone, the sludge structure underwent disruption due to the dissolution of TB-EPS. Consequently, finer flocs formed compared to the original sludge (Fig. 7b and c). Unfortunately, these finer sludges tended to clog the filter cloth, posing a greater challenge to sludge dewatering. Conversely, when $FeCl_3$ was added alone, the sludge particle size increased and became more uniform

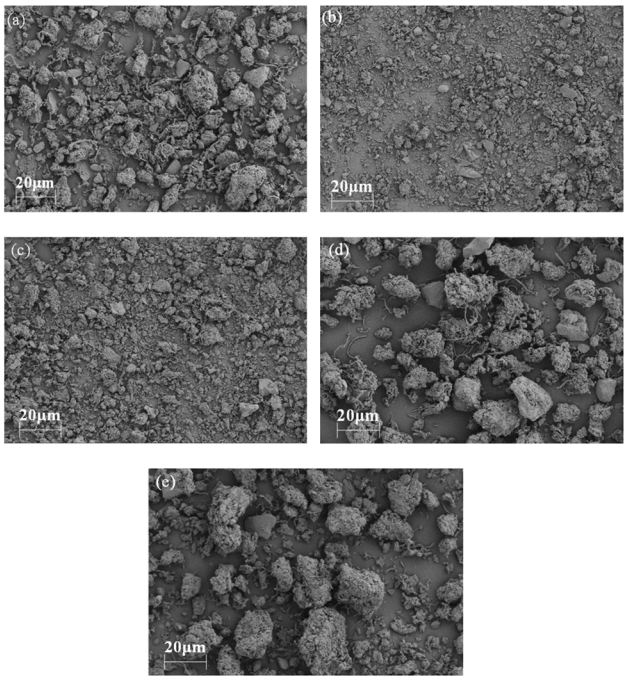

Fig. 7 Changes in sludge morphology under various conditions: (a) original sludge, (b) PDMDAAC alone, (c) HCl alone, (d) $FeCl_3$ alone, and (e) PDMDAAC + $FeCl_3$ + HCl.

(Fig. 7d), confirming its flocculation properties. Despite the increase in size when dosing $FeCl_3$ alone, these larger sludges still retained a substantial amount of bound water interacting with EPS. Consequently, achieving effective dewatering performance solely through $FeCl_3$ addition proved challenging. However, after conditioning with the composite conditioner (PDMDAAC + $FeCl_3$ + HCl), notable improvements were observed (Fig. 7e). The sludge not only formed larger particle sizes but, more importantly, released a significant amount of bound water. This release included bound water interacting with EPS as well as intracellular bound water after cell lysis, both contributing positively to enhanced sludge dewatering.

3.4. Possible mechanisms of sludge dewatering

In this study, a comprehensive approach to deep dehydration was employed using PDMDAAC, $FeCl_3$, and HCl as conditioners. The results demonstrated that all three conditioners effectively dissolved EPS and destabilized the sludge by reducing the zeta potential. However, their primary roles differed: PDMDAAC primarily dissolved TB-EPS, releasing a portion of the bound water. Nevertheless, this led to the destruction of the sludge structure, resulting in the formation of finer sludge and an increase in viscosity. In contrast, $FeCl_3$ predominantly acted as a flocculant, promoting the aggregation of fine sludge particles to form larger sizes. HCl, on the other hand, contribute to the dissolution of TB-EPS, leading to the release of substantial bound water. Additionally, the acidic pH induced by HCl played a role in reducing the viscosity of the sludge.

In summary, the sludge dewatering mechanisms in this study can be outlined as follows: first, the addition of

PDMDAAC dissolved and decomposed TB-EPS, releasing bound water. Secondly, $FeCl_3$ facilitated the reconstruction of fine sludge into a stable, larger particle size structure, reducing bound water. Finally, the addition of HCl induced cell lysis, releasing bound water, and transformed TB-EPS into S-EPS, further releasing bound water. Consequently, HCl addition maximized the release of bound water while maintaining a large sludge particle size. In summary, the quantity of TB-EPS and sludge particle size emerged as key factors influencing sludge deep dehydration. PN in TB-EPS played a major role in sludge dewatering, with the N–H functional group identified as the key factor affecting the water-holding properties of EPS.

3.5. Significance of sludge dewatering using PDMDAAC and $FeCl_3$ under acidic condition

The large amount of waste sludge produced by the activated sludge process must be dewatered before final disposal. In this study, deep sludge dewatering was achieved under acidic condition through the use of PDMDAAC and $FeCl_3$ as conditioning agents. Compared with conventional agents (polymeric $FeCl_3$, polymeric aluminum chloride, and polyacrylamide *etc.*) that reduce sludge MC to 80%, this study can reduce the volume of sludge by half, and therefore, storage and transportation costs can be reduced by 50% or more. In addition, if the sludge is subsequently disposed of by incineration, the combustion calorific value can be enhanced by more than 20%. Therefore, this study provides a new idea for sludge reduction treatment and disposal. However, the process of sludge dewatering inevitably introduces chemical reagents into the sludge dewatering solution, especially the impact of PDMDAAC on the environment is still unclear, which will be a limiting factor for the application of this method.

4. Conclusions

In this study, deep sludge dewatering at pH 3 was achieved through the use of PDMDAAC and $FeCl_3$ as conditioning agents. Further analysis revealed a remarkable 70% reduction in the TB-EPS of the conditioned sludge, with the diminished fractions primarily consisting of PNs, specifically tryptophan and tyrosine proteins. Simultaneously, the absorption peaks of N–H and C=C in TB-EPS saw a significant decrease. These findings highlight the importance of substantial TB-EPS reduction in enhancing sludge dewatering performance, with the N–H group in PNs identified as the key factor influencing the water-holding capacity of EPS. Furthermore, the particle size also plays a critical role in sludge dewatering. PDMDAAC contributes to a finer sludge, $FeCl_3$ causes these fine particles to aggregate into larger sizes, and hydrochloric acid maximizes the release of bound water while maintaining the large particle size. This study presents an alternative method for achieving deep dewatering of residual sludge.

Conflicts of interest

There were no conflicts to declare.

Acknowledgements

This work was supported by the Shaanxi Province key industry chain (group) project [Grant number 2022ZDLSF06-05], Shaanxi Province Key R&D Program Project [Grant number 2023-YBSF-596] and the Science and Technology Innovative Team Plan of Shaanxi Province [Grant number 2024RS-CXTD-51].

Notes and references

1 Z.-j Xu, J. Zhou, Y.-D. Liu, L.-F. Gu, J. Xu, C. Wu and X.-Y. Zhang, *RSC Adv.*, 2018, **8**, 38574–38581.
2 L. Świerczek, B. M. Cieślik and P. Konieczka, *J. Cleaner Prod.*, 2018, **200**, 342–356.
3 N. Lin, W. Zhu, X. Fan, C. Wang, C. Chen, H. Zhang, L. Chen, S. Wu and Y. Cui, *Chemosphere*, 2020, **249**, 126108.
4 W. Yu, Y. Wan, Y. Wang, Y. Zhu, S. Tao, Q. Xu, K. Xiao, S. Liang, B. Liu, H. Hou, J. Hu and J. Yang, *Environ. Res.*, 2021, **196**, 110328.
5 X. Cao, R. He and M. Jia, *Environ. Res.*, 2023, **239**, 117226.
6 J. Hu, Z. Li, A. Zhang, S. Mao, I. R. Jenkinson and W. Tao, *Environ. Res.*, 2020, **188**, 109764.
7 X. Zhou, W. Jin, H. Chen, C. Chen, S. Han, R. Tu, W. Wei, S.-H. Gao, G.-J. Xie and Q. Wang, *Water Sci. Technol.*, 2017, **76**(9), 2427–2433.
8 B. Cao, T. Zhang, W. Zhang and D. Wang, *Water Res.*, 2021, **189**, 116650.
9 Y.-H. Zhou, H.-L. Zheng, B.-Y. Gao, Y.-P. Guab, X. Li, Z.-B. Liu and A. M. Jiménez, *RSC Adv.*, 2017, **7**, 28733–28745.
10 H. Wei, J. Ren, A. Li and H. Yang, *Chem. Eng. J.*, 2018, **349**, 737–747.
11 D.-Q. He, H.-W. Luo, B.-C. Huang, C. Qian and H.-Q. Yu, *Bioresour. Technol.*, 2016, **218**, 526–532.
12 Q. Zhang, G. Cui, X. He, Z. Wang, T. Tang, Q. Zhao and Y. Liu, *Environ. Res.*, 2022, **212**, 113490.
13 S. He, L. Feng, W. Zhao, J. Li, Q. Zhao and L. Wei, *Chem. Eng. J.*, 2023, **462**, 142234.
14 W. Bi, M. Chen, C. Hu, H. Sun, S. Xu, J. Jiang, L. Wang, X. Li and J. Deng, *J. Environ. Manage.*, 2023, **344**, 118450.
15 H.-J. Kim, K. Chon, Y.-G. Lee, Y.-K. Kim and A. Jang, *Environ. Res.*, 2020, **188**, 109746.
16 D. He, M. Sun, B. Bao, J. Chen, H. Luo and J. Li, *J Water Process Eng.*, 2022, **47**, 102744.
17 B. Wu, X. Dai and X. Chai, *Water Res.*, 2020, **180**, 115912.
18 L.-F. Wang, L.-L. Wang, W.-W. Li, D.-Q. He, H. Jiang, X.-D. Ye, H.-P. Yuan, N.-W. Zhu and H.-Q. Yu, *Chem. Eng. Sci.*, 2014, **116**, 228–234.
19 A. Li, C. Huang, X. Feng, Y. Li, H. Yang, S. Wang and J. Li, *Environ. Res.*, 2022, **211**, 113024.
20 M. Basuvaraj, J. Fein and S. N. Liss, *Water Res.*, 2015, **82**, 104–117.
21 J. Xing, Q. Tang, M. Gan, Z. Ji, X. Fan, Z. Sun and X. Chen, *J. Environ. Manage.*, 2023, **332**, 117403.
22 D.-Q. He, J.-Y. Chen, B. Bao, X.-L. Pan, J. Li, C. Qian and H.-Q. Yu, *J. Environ. Sci.*, 2020, **88**, 21–30.
23 C. Feng, T. Lotti, R. Canziani, Y. Lin, C. Tagliabue and F. Malpei, *Sci. Total Environ.*, 2021, **753**, 142051.

24 Z. Wei, D. Li, S. Li, T. Hao, H. Zeng and J. Zhang, *Bioresour. Technol.*, 2023, **370**, 128558.
25 W. Yang, L. Cheng, H. Liang, A. Xu, Y. Li, M. Nabi, H. Wang, J. Hu and D. Gao, *J. Environ. Manage.*, 2023, **344**, 118460.
26 S. Getahun, S. Septien, J. Mata, T. Somorin, I. Mabbett and C. Buckley, *J. Environ. Manage.*, 2020, **261**, 110267.
27 L.-F. Wang, C. Qian, J.-K. Jiang, X.-D. Ye and H.-Q. Yu, *Environ. Pollut.*, 2017, **231**, 1388–1392.
28 P. H. Nielsen, B. K. Frølund and K. Keiding, *Appl. Microbiol. Biotechnol.*, 1996, **44**, 823–830.
29 Y.-T. Lv, X. Chen, X. Zhang, Y. Li, Q. Lv, R. Miao, L. Nie and L. Wang, *Chem. Eng. J.*, 2023, **454**, 140314.
30 Z. Chen, W. Zhang, D. Wang, T. Ma and R. Bai, *Water Res.*, 2015, **83**, 367–376.
31 D. Ge, Y. Dong, W. Zhang, H. Yuan and N. Zhu, *Sci. Total Environ.*, 2020, **733**, 139146.
32 Z. Wang, H. Song, L. Song, Z. Yin, K. Hui, W. Gao and L. Xuan, *Chemosphere*, 2022, **306**, 135484.
33 M. Citeau, O. Larue and E. Vorobiev, *Water Res.*, 2011, **45**(6), 2167–2180.
34 J. Yu, K. Xiao, H. Xu, Y. Li, Q. Xue, W. Xue, A. Zhang, X. Wen, G. Xu and X. Huang, *Water Res.*, 2023, **235**, 119866.
35 E. Neyens, J. Baeyens, R. Dewil and B. De Heyder, *J. Hazard. Mater.*, 2004, **106**(2), 83–92.
36 R. Zhang, Y. Mao and L. Meng, *Sep. Purif. Technol.*, 2021, **276**, 119359.
37 N. Chen, S. Tao, K. Xiao, S. Liang, J. Yang and L. Zhang, *Chemosphere*, 2020, **238**, 124598.
38 Y. Liu and H. H. P. Fang, *Crit. Rev. Environ. Sci. Technol.*, 2003, **33**(3), 237–273.
39 Y. Zhang, B. Cao, R. Ren, Y. Shi, J. Xiong, W. Zhang and D. Wang, *Sci. Total Environ.*, 2021, **801**, 149753.
40 H. Li, J. Chen, J. Zhang, T. Dai, H. Yi, F. Chen, M. Zhou and H. Hou, *J. Environ. Manage.*, 2022, **316**, 115210.
41 K. Xiao, K. Pei, H. Wang, W. Yu, S. Liang, J. Hu, H. Hou, B. Liu and J. Yang, *Water Res.*, 2018, **140**, 232–242.
42 K. Xiao, G. Abbt-Braun and H. Horn, *Water Res.*, 2020, **187**, 116441.
43 Y. Chen, F. Bai, Z. Li, P. Xie, Z. Wang, X. Feng, Z. Liu and L.-Z. Huang, *Chem. Eng. J.*, 2020, **383**, 123165.
44 H. Wei, Y. Tang, A. Li and H. Yang, *Chemosphere*, 2019, **227**, 269–276.
45 M. Raynaud, J. Vaxelaire, J. Olivier, E. Dieudé-Fauvel and J.-C. Baudez, *Water Res.*, 2012, **46**(14), 4448–4456.
46 B. Wu, H. Wang, W. Li, X. Dai and X. Chai, *Water Res.*, 2022, **213**, 118169.
47 X. Liu, Y. Zhai, Z. Xu, L. Liu, W. Ren, Y. Xie, C. Li, Y. Zhu and M. Xu, *Chem. Eng. J.*, 2023, **457**, 141106.
48 L. Yuan, Y. Li, T. Zeng, D. Wang, X. Liu, Q. Xu, Q. Yang, F. Yang and H. Chen, *Chem. Eng. J.*, 2021, **411**, 128465.
49 X. Y. Cao, Q. Y. Yue, L. Y. Song, M. Li and Y. C. Zhao, *J. Hazard. Mater.*, 2007, **147**(1), 133–138.
50 S. Hu, J. Hu, B. Liu, D. Wang, L. Wu, K. Xiao, S. Liang, H. Hou and J. Yang, *Water Res.*, 2018, **145**, 162–171.
51 M. S. Kim, K.-M. Lee, H.-E. Kim, H.-J. Lee, C. Lee and C. Lee, *Environ. Sci. Technol.*, 2016, **50**(13), 7106–7115.
52 R. Deng, J. Lai, Z. Liu, B. Song, H. Liu, D. Chen, G. Zuo, Z. Yang, F. Meng, T. Gong and M. Song, *Chemosphere*, 2023, **326**, 138443.